Submitted to ApJ

Neutrino Annihilation between Binary Neutron Stars

Jay D. Salmonson

James R. Wilson

Lawrence Livermore National Laboratory, Livermore, CA 94550

ABSTRACT

We calculate the neutrino pair annihilation rate into electron pairs between two neutron stars in a binary system. We present a closed formula for the energy deposition rate at any point between the stars, where each neutrino of a pair derives from each star, and compare this result to that where all neutrinos derive from a single neutron star. An approximate generalization of this formula is given to include the relativistic effects of gravity. We find that this inter-star neutrino annihilation is a significant contributor to the energy deposition between heated neutron star binaries. In particular, for two neutron stars near their last stable orbit, inter-star neutrino annihilation energy deposition is almost equal to that of single star energy deposition.

Subject headings: gamma rays: bursts — gamma rays: theory

1. Introduction

Neutrino emission from, and interactions above neutron stars has long been understood to be an important process in supernovae (e.g. Wilson & Mayle 1993). One interaction of particular interest is neutrino annihilation: $\nu+\overline{\nu} \rightarrow e^+ + e^-$ because it converts neutrinos into electrons, which, due to their vastly larger cross-section, are an important source of energy for supernovae and possibly gamma-ray bursts. Because of the strong gravity of neutron stars, relativistic effects must be included when calculating neutrino processes. Rates of the $\nu\overline{\nu} \rightarrow e^+e^-$ interaction above a neutron star were originally calculated without gravity by Cooperstein et al. (1987) and Goodman et al. (1987). In Salmonson & Wilson (1999) these neutrino annihilation rates were calculated with gravity and it was found that general relativistic effects significantly augmented the efficiency; by up to a factor of four for supernovae and up to a factor of thirty for lone neutron stars at their critical density.

Another situation where neutrino emission from neutron stars is important is in neutron star binary (NSB) systems. Binary neutron star mergers have long been a possible progenitor for gamma-ray bursts (GRBs) (e.g. Eichler et al. 1989; Mészáros & Rees 1992). In particular, current trends would suggest that NSBs may be the progenitor of the "short" GRBs, characterized by timescales $\lesssim 1$ second, which are thought to be distinct from the class of "long" GRBs (e.g. Fryer et al. 1999). As such, we are moved to study mechanisms for energy extraction.

Due to the extreme high densities inside the neutron stars, neutrinos, with their small cross-section, are a necessary component of the energetics of supernovae and compact binary merger scenarios. In particular, only a small proportion ($\sim 1\%$) of the total energy (which could be as high as the binding energy of a solar mass neutron star) in neutrinos need be transferred to conventional matter in order to produce large, observable, energetic events. Such a mechanism has been suggested as an energy source for GRBs by Salmonson et al. (2001); Wilson et al. (1997); Mészáros & Rees (1992); Eichler et al. (1989).

In this paper we study the inter-star neutrino annihilation; where each neutrino in an annihilation pair derives from each star in the binary. This is distinct from the single star neutrino annihilation discussed in Salmonson & Wilson (1999). Both processes will occur in a binary star system and will sum to give the total energy depostion from neutrino annihilation. We will compare and contrast the contributions of these two processes. We find that the inter-star component is a very significant contributor to the total energy deposition. In Section 2 we derive the results without general relativistic effects. In Section 3 we make some estimates of the augmentation of annihilation due to general relativity and compare with the relativistic augmentation derived in Salmonson & Wilson (1999) for the single star case.

2. Interstar Neutrino Annihilation

Starting from references in Salmonson & Wilson (1999), the energy deposition via neutrino-antineutrino annihilation into electron-positron pairs per unit time per unit volume is

$$\dot{q} = \frac{DG_F^2}{3\pi c^5}\Theta(\vec{r}) \iint f_\nu f_{\overline{\nu}}(\varepsilon_\nu + \varepsilon_{\overline{\nu}})\varepsilon_\nu^3 d\varepsilon_\nu \varepsilon_{\overline{\nu}}^3 d\varepsilon_{\overline{\nu}} \ , \tag{1}$$

where f_ν and $f_{\overline{\nu}}$ are the respective neutrino and anti-neutrino number densities in phase space, ε_ν and $\varepsilon_{\overline{\nu}}$ are their energies, $\Theta(\vec{r})$ is the integral over incident neutrino angles, $G_F^2 =$

5.29×10^{-44} cm^2 MeV^{-2} and

$$D = 1 \pm 4\sin^2\theta_W + 8\sin^4\theta_W \ , \tag{2}$$

where the + sign is for $\nu_e\overline{\nu}_e$ pairs, while − is for $\nu_\mu\overline{\nu}_\mu$ and $\nu_\tau\overline{\nu}_\tau$ pairs. We assume black-body-like neutrino emission; a good assumption for thermal neutrinos diffusing out of a hot neutron star (Wilson et al. 1996). Neglecting redshift effects on the temperature for the moment, eqn. (1) reduces to

$$\dot{q} = 7.97 \times 10^{21} D \left(\frac{T}{1\mathrm{MeV}}\right)^9 \Theta(\vec{r}) \text{ ergs cm}^{-3} \text{ sec}^{-1} \tag{3}$$

where $D = 1.23$ for $\nu_e\overline{\nu}_e$ pairs and otherwise $D = 0.814$. The integration over incident neutrino angles is

$$\Theta(\vec{r}) \equiv \iint (1 - \mathbf{\Omega}_\nu \cdot \mathbf{\Omega}_{\overline{\nu}})^2 d\Omega_\nu d\Omega_{\overline{\nu}} \ . \tag{4}$$

We define the neutrino trajectories, in (x, y, z), from star 1 (on the left) as

$$\mathbf{\Omega}_1 = (\cos\theta_1', \ \sin\theta_1'\cos\phi_1', \ \sin\theta_1'\sin\phi_1') \tag{5}$$

and for star 2 (on the right) as (note that $x \to -x$ do to reflection symmetry)

$$\mathbf{\Omega}_2 = (-\cos\theta_2', \ \sin\theta_2'\cos\phi_2', \ \sin\theta_2'\sin\phi_2') \tag{6}$$

where (θ_1', ϕ_1') and (θ_2', ϕ_2') are the direction angles for the neutrino trajectories in spherical coordinates from stars 1 and 2 respectively, so that $(\theta_i' = 0, \phi_i' = 0)$ points to the center of star $i = 1, 2$. Since we wish to evaluate the integral of eqn. (4) at any point in space around the stars, we rotate the vector $\mathbf{\Omega}_1$ by an angle Θ_1

$$\mathbf{\Omega}_1 = (\cos\theta_1'\cos\Theta_1 - \sin\theta_1'\cos\phi_1'\sin\Theta_1, \ \sin\theta_1'\cos\phi_1'\cos\Theta_1 + \cos\theta_1'\sin\Theta_1, \ \sin\theta_1'\sin\phi_1') \ . \tag{7}$$

A rotation of $\mathbf{\Omega}_2$ by Θ_2 gives (note that $\mathbf{\Omega}_2$ will have the same form as $\mathbf{\Omega}_1$ except $x \to -x$)

$$\mathbf{\Omega}_2 = (-\cos\theta_2'\cos\Theta_2 + \sin\theta_2'\cos\phi_2'\sin\Theta_2, \ \sin\theta_2'\cos\phi_2'\cos\Theta_2 + \cos\theta_2'\sin\Theta_2, \ \sin\theta_2'\sin\phi_2') \ . \tag{8}$$

Thus, noting $(1 - \mathbf{\Omega}_1 \cdot \mathbf{\Omega}_2)^2 = 1 - 2\mathbf{\Omega}_1 \cdot \mathbf{\Omega}_2 + (\mathbf{\Omega}_1 \cdot \mathbf{\Omega}_2)^2$ and $d\Omega_i = \sin\theta_i' d\theta_i' d\phi_i'$ where $i = 1, 2$, eqn. (4) can be integrated and becomes

$$\Theta_{\rm inter}(\theta_1,\theta_2,\Theta_1,\Theta_2) = (\pi^2(516 + 8\cos[\theta_1] + 4\cos[2\theta_1] + 4\cos[\theta_1 - 2\theta_2] + 8\cos[\theta_1 - \theta_2] + 2\cos[2(\theta_1 - \theta_2)]$$
$$+ 4\cos[2\theta_1 - \theta_2] + 8\cos[\theta_2] + 4\cos[2\theta_2] + 8\cos[\theta_1 + \theta_2] + 2\cos[2(\theta_1 + \theta_2)] + 4\cos[2\theta_1 + \theta_2]$$
$$+ 4\cos[\theta_1 + 2\theta_2] + 12\cos[\theta_1 - 2\Theta_1 - \theta_2 - 2\Theta_2] + 6\cos[2\theta_1 - 2\Theta_1 - \theta_2 - 2\Theta_2]$$
$$+ 12\cos[\theta_1 - 2\Theta_1 + \theta_2 - 2\Theta_2] + 6\cos[2\theta_1 - 2\Theta_1 + \theta_2 - 2\Theta_2] + 96\cos[\theta_1 - \Theta_1 - \Theta_2]$$
$$+ 6\cos[2(\theta_1 - \Theta_1 - \Theta_2)] + 48\cos[\theta_1 - \Theta_1 - \theta_2 - \Theta_2] + 3\cos[2(\theta_1 - \Theta_1 - \theta_2 - \Theta_2)]$$
$$+ 48\cos[\theta_1 - \Theta_1 + \theta_2 - \Theta_2] + 3\cos[2(\theta_1 - \Theta_1 + \theta_2 - \Theta_2)] + 192\cos[\Theta_1 + \Theta_2] + 12\cos[2(\Theta_1 + \Theta_2)]$$
$$+ 96\cos[\theta_1 + \Theta_1 + \Theta_2] + 6\cos[2(\theta_1 + \Theta_1 + \Theta_2)] + 96\cos[\Theta_1 - \theta_2 + \Theta_2] + 6\cos[2(\Theta_1 - \theta_2 + \Theta_2)]$$
$$+ 48\cos[\theta_1 + \Theta_1 - \theta_2 + \Theta_2] + 3\cos[2(\theta_1 + \Theta_1 - \theta_2 + \Theta_2)] + 96\cos[\Theta_1 + \theta_2 + \Theta_2]$$
$$+ 6\cos[2(\Theta_1 + \theta_2 + \Theta_2)] + 48\cos[\theta_1 + \Theta_1 + \theta_2 + \Theta_2] + 3\cos[2(\theta_1 + \Theta_1 + \theta_2 + \Theta_2)]$$
$$+ 12\cos[2\Theta_1 - \theta_2 + 2\Theta_2] + 12\cos[\theta_1 + 2\Theta_1 - \theta_2 + 2\Theta_2] + 6\cos[2\theta_1 + 2\Theta_1 - \theta_2 + 2\Theta_2]$$
$$+ 12\cos[2\Theta_1 + \theta_2 + 2\Theta_2] + 12\cos[\theta_1 + 2\Theta_1 + \theta_2 + 2\Theta_2] + 6\cos[2\theta_1 + 2\Theta_1 + \theta_2 + 2\Theta_2]$$
$$+ 12\cos[\theta_1 - 2(\Theta_1 + \Theta_2)] + 12\cos[\theta_1 + 2(\Theta_1 + \Theta_2)] + 6\cos[\theta_1 - 2(\Theta_1 - \theta_2 + \Theta_2)]$$
$$+ 6\cos[\theta_1 + 2(\Theta_1 - \theta_2 + \Theta_2)] + 6\cos[\theta_1 - 2(\Theta_1 + \theta_2 + \Theta_2)]$$
$$+ 6\cos[\theta_1 + 2(\Theta_1 + \theta_2 + \Theta_2)])\sin^2[\theta_1/2]\sin^2[\theta_2/2])/24 \ . \tag{9}$$

An illustration of the geometry is shown in Figure 1. Specifically, θ_i is the apparent radial angular size of star i and Θ_i is the angle star i is observed at with respect to the axis connecting the star centers. It is useful to convert eqn. (9) to cartesian coordinates ($\Theta(\theta_1,\theta_2,\Theta_1,\Theta_2) \rightarrow \Theta(x,y)$) via the following substitutions. If two stars of mass M and radius R are separated by distance d, so the half-separation is $d_2 \equiv d/2$ and

$$r_{1,2} \equiv \sqrt{(d_2 \pm x)^2 + y^2} \ , \tag{10}$$

then

$$\theta_{1,2} = \arcsin\left(\frac{R}{r_{1,2}}\right) \tag{11}$$

$$\Theta_{1,2} = \arctan\left(\frac{y}{d_2 \pm x}\right) \tag{12}$$

where the + and − signs correspond to stars to the left (star 1) and right (star 2) of the axis of symmetry respectively. Figure 2 shows a contour plot of this integration over inter-star incident neutrino angles given by eqns. (9, 11, 12). As expected, $\nu\overline{\nu}$ annihilation takes place primarily between the stars, where the cross-section and flux are highest.

For comparison, the result for a single neutron star is (Salmonson & Wilson 1999)

$$\Theta(r)_{\rm single} = \frac{2\pi^2}{3}(1-x)^4(x^2+4x+5) \tag{13}$$

where r is the distance from the neutron star center and, for a star of mass M and radius R, we define

$$x \equiv \sqrt{1-\left(\frac{R}{r}\right)^2 \frac{1-\frac{2M}{r}}{1-\frac{2M}{R}}} \ . \tag{14}$$

This equation (14) takes into account the effects of general relativity in Schwarzchild coordinates. In particular, the gravitational bending of neutrino trajectories (see Section 3). For the Newtonian result, take $M = 0$. In Figure 3 is shown a comparison between $\Theta_{\rm inter}$ (eqn. 9) and $\Theta_{\rm single}$ (eqn. 13) along the axis between the stars. We see that annihilation of $\nu\overline{\nu}$ from a single star is dominant near the stellar surfaces, while inter-star annihilation is important between the stars.

One can compare the rate of inter-star deposition to single star deposition. A key conclusion of this paper is that the inter-star annihilation is a significant component of the total energy deposition. In Figure 4 we see a ratio of total energy deposited via inter-star annihilation versus that for a single star over a range of stellar separations. The total energy deposited is an integral of eqn. (3) over the interstellar volume V

$$\dot{Q}_{\rm Newt} \equiv \int \dot{q}\ dV \propto \int \Theta\ dV \ . \tag{15}$$

We see that in this Newtonian limit $\dot{Q}_{\rm inter}/\dot{Q}_{\rm single} \sim 80\%$ for close separations (i.e. $d_2 < 2R$) where $\dot{Q}_{\rm inter} \propto \int \Theta_{\rm inter}\ dV$ using eqn. (9) and $\dot{Q}_{\rm single} \propto \int \Theta_{\rm single}\ dV$ using eqn. (13).

3. General Relativity

Analytical calculation of the general relativistic effects on inter-star neutrino annihilation is extremely complex. Instead, we make some crude approximations to gain some insight into the effect of gravity. We neglect possible rotation effects. It is most convenient and intuitive to use isotropic coordinates

$$ds^2 = -\alpha^2 dt^2 + \phi^4(d\overline{r}^2 + \overline{r}^4 d\Omega^2) \tag{16}$$

where, for one star (Misner et al. 1973)

$$\begin{aligned} \alpha &= \frac{1-\frac{M}{2\overline{r}}}{1+\frac{M}{2\overline{r}}} \\ \phi &= 1+\frac{M}{2\overline{r}} \end{aligned} \tag{17}$$

and the isotropic distance, $\overline{r}$, to the center of the star is related to the Schwarzchild distance r by

$$r = \overline{r}\left(1+\frac{M}{2\overline{r}}\right)^2 = \overline{r}\phi(\overline{r})^2 \ . \tag{18}$$

In the two star environment we define

$$\begin{aligned} \alpha(\overline{r}_+,\overline{r}_-) &\equiv 1-\frac{M}{\overline{r}_+}-\frac{M}{\overline{r}_-} \\ \phi(\overline{r}_+,\overline{r}_-) &\equiv 1+\frac{M}{2\overline{r}_+}+\frac{M}{2\overline{r}_-} \end{aligned} \tag{19}$$

where r_+ (r_-) indicates the distance to the center of the star on the left (right). This choice of metric is found to be an adequate approximation, to a few percent, of the real metric as numerically calculated by Wilson et al. (1996). The value of these metric components at the stellar surface is not at constant potential (because we neglect tidal distortions which equalize the surface potential), thus we define the potentials at the surface to be

$$\alpha_s \equiv \alpha(\overline{R},d_s) \ , \ \phi_s \equiv \phi(\overline{R},d_s) \tag{20}$$

with

$$d_s \equiv \frac{\overline{R}}{r_\mp}\sqrt{\left(d_2\big(2\frac{r_\mp}{\overline{R}}-1\big)\pm x\right)^2+y^2} \tag{21}$$

using eqn. (10) and where one chooses the upper sign if $x>0$ and vice versa. This corresponds to the potential at the surface of the star at the point for which the line to point (x,y) is perpendicular to the surface. From here on we simplify the notation by suppressing the metric arguments (e.g. $\alpha \equiv \alpha(\overline{r}_+,\overline{r}_-)$).

For the single star case, in these coordinates, eqn. (14) becomes

$$x = \sqrt{1-\left(\frac{\overline{R}}{\overline{r}}\right)^2\left(\frac{\phi_s}{\phi}\right)^3\left(\frac{\alpha}{\alpha_s}\right)^2} \tag{22}$$

where $\overline{R}$ is the isotropic stellar radius. For compact neutron stars near collapse, we will take $\overline{R} = 7.5$ km (Wilson et al. 1996).

For the inter-star case, the apparent radial angular size, θ, of a star will be augmented due to the gravitational bending of neutrino geodesics by the mass of the star. We include this effect by modifying eqn. (11) by identifying $R \rightarrow \overline{R}\phi_s^{3/2}/\alpha_s$ and $r \rightarrow \overline{r}\phi^{3/2}/\alpha$ from eqn. (22). These substitutions take into account the "lensing" effect due to the gravitational bending of the neutrino geodesics (Salmonson & Wilson 1999) and give

$$\theta_\pm \equiv \arcsin\left(\frac{\overline{R}}{\overline{r}_\pm}\left(\frac{\phi_s}{\phi}\right)^{3/2}\left(\frac{\alpha}{\alpha_s}\right)\right) . \tag{23}$$

In addition, there will be a redshift (or blueshift) of the neutrino energies. Specifically, assuming the neutrinos emerge from the neutrinosphere of each star with surface temperature T_s, then the temperature at a position (x, y), using eqn. (10), is

$$T(\overline{r}_+, \overline{r}_-) = \frac{\alpha_s}{\alpha} T_s . \tag{24}$$

Then the energy deposited at this point is (eqn. 3)

$$\dot{q} = 7.97 \times 10^{21} D \left(\frac{T(\vec{r})}{1\mathrm{MeV}}\right)^9 \Theta(\vec{r}) \text{ ergs cm}^{-3} \text{ sec}^{-1} \propto \left(\frac{\alpha_s}{\alpha} T_s\right)^9 \Theta(\vec{r}) . \tag{25}$$

Following Salmonson & Wilson (1999) we define the total energy deposition

$$\dot{Q}_{\mathrm{GR}} \equiv \int \dot{q} dV = 7.97 \times 10^{21} D \left(\frac{\alpha_s T_s}{1\mathrm{MeV}}\right)^9 \int \frac{\Theta(\vec{r})}{\alpha^9} \phi^6 dx^3 \text{ ergs sec}^{-1} \tag{26}$$

where the metric is given by eqn. (19) and the inter-star angle factor is calculated using eqns. (9, 12, 23) and the single star angle factor is given by eqns. (13, 22). A comparison of these two rates for several stellar masses and a range of separations is shown in Figure 5. One can see that as the stars approach their last stable orbit, $d_2 \sim 10-12$ km (Mathews & Wilson 2000), the inter-star contribution to neutrino energy deposition, $\dot{Q}_{\mathrm{inter}}$ becomes comparable to the single star contribution $\dot{Q}_{\mathrm{single}}$. Thus the inter-star energy deposition is significant for hot neutron stars in close binaries. In Figure 6 is shown the augmentation of both inter-star, $\dot{Q}_{\mathrm{inter}}$, and single star, $\dot{Q}_{\mathrm{single}}$, energy depositions for a typical half-separation, $d_2 = 15$ km, and a range of masses. These are compared with the energy deposition for an isolated neutron star, $\dot{Q}_{\mathrm{one\ star}}$, (Salmonson & Wilson 1999) here presented in isotropic coordinates.

4. Discussion

Herein we have calculated the inter-star neutrino annihilation rate for close neutron stars of equal mass in a binary system. A generalization of interest would be the consideration of systems with stars of unequal mass. While a detailed calculation of such is difficult and beyond the capability of the analytical results presented here, we can argue that, at least for small departures from mass equality, the inter-star annihilation rate will not change much. In the stellar compression effect discussed by (Mathews & Wilson 2000), the larger of the two unequal mass stars may be thought to receive larger compression due to its excess mass. From the results given in tables III and IV of Mathews & Wilson (2000) is found that the compression for a given four-velocity is quadratic in mass. However, the smaller mass star will move faster, varying inversely with mass, and compression is shown to scale quadratically with four-velocity (Mathews & Wilson 2000). Therefore we expect that there will be a balancing effect keeping the stars at approximately equal temperatures and thus we expect the energy deposition of eqn. (3), which scales like $\propto T^9$, to be roughly constant for stars differing in mass by 5 %, which is a reasonable range for observed neutron star binaries.

In conclusion, we find that inter-star neutrino annihilation is a significant component of the total neutrino annihilation in a neutron star binary system and will thus be a major contributor to the available energy of coallescing binary systems. We provide formulas for calculating this energy deposition. Future work will use 3-D relativistic hydrodynamic calculations to take this effect into account and thus improve the calculations of Salmonson et al. (2001). In particular the inter-star annihilation will lead to non-isotropic outflow.

This work was performed under the auspices of the U.S. Department of Energy by University of California Lawrence Livermore National Laboratory under contract W-7405-ENG-48.

REFERENCES

Cooperstein J., Van Den Horn L. J., Baron E. 1987, ApJ, 321, L129

Eichler D., Livio M., Piran T., Schramm D. N. 1989, Nat, 340, 126

Fryer C. L., Woosley S. E., Hartmann D. H. 1999, ApJ, 526, 152

Goodman J., Dar A., Nussinov S. 1987, ApJ, 314, L7

Mathews G. J., Wilson J. R. 2000, Phys. Rev. D, 61, 127304

Mészáros P., Rees M. J. 1992, ApJ, 397, 570

Misner C. W., Thorne K. S., Wheeler J. A. 1973, Gravitation, W. H. Freeman, San Francisco

Salmonson J. D., Wilson J. R. 1999, ApJ, 517, 859

Salmonson J. D., Wilson J. R., Mathews G. J. 2001, ApJ, 553, 471

Wilson J. R., Mathews G. J., Marronetti P. 1996, Phys. Rev. D, 54, 1317

Wilson J. R., Mayle R. W. 1993, Phys. Rep., 227, 97

Wilson J. R., Salmonson J. D., Mathews G. J. 1997, in C. A. Meegan, R. D. Preece, T. M. Koshut (eds.), Fourth Huntsville Gamma-Ray Burst Symposium, held 15-20 September, 1997., American Institute of Physics, p. 788

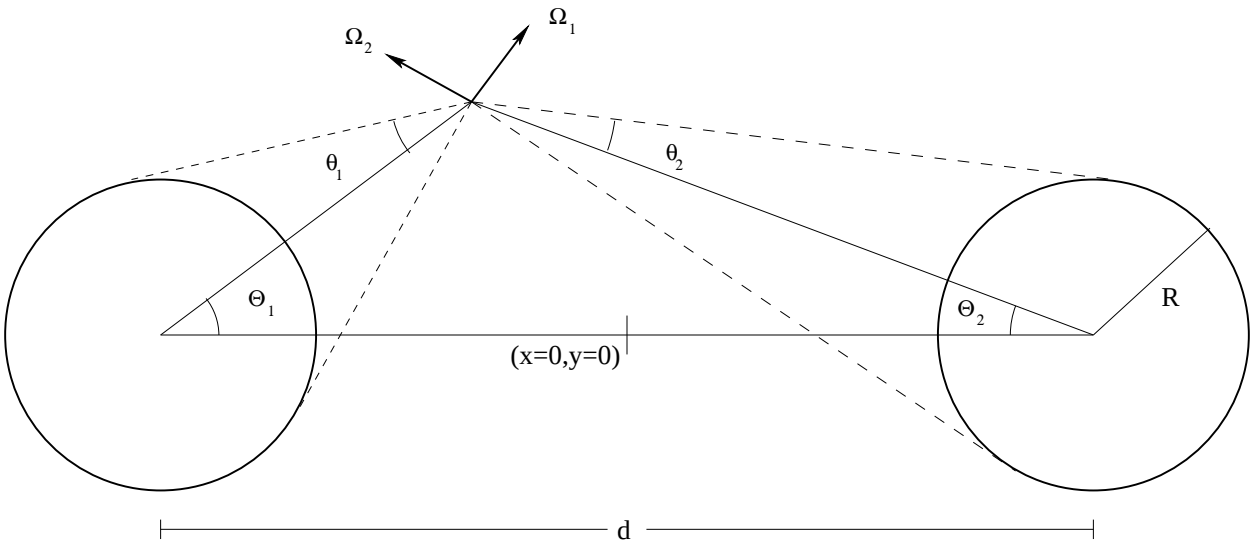

Fig. 1.— Diagram representing the geometry and defining quantities used in Eqns (9, 11, 12). For clarity, this illustration shows only the special case where the neutrino trajectories are coplanar (i.e. $\phi_1 = \phi_2 = 0$).

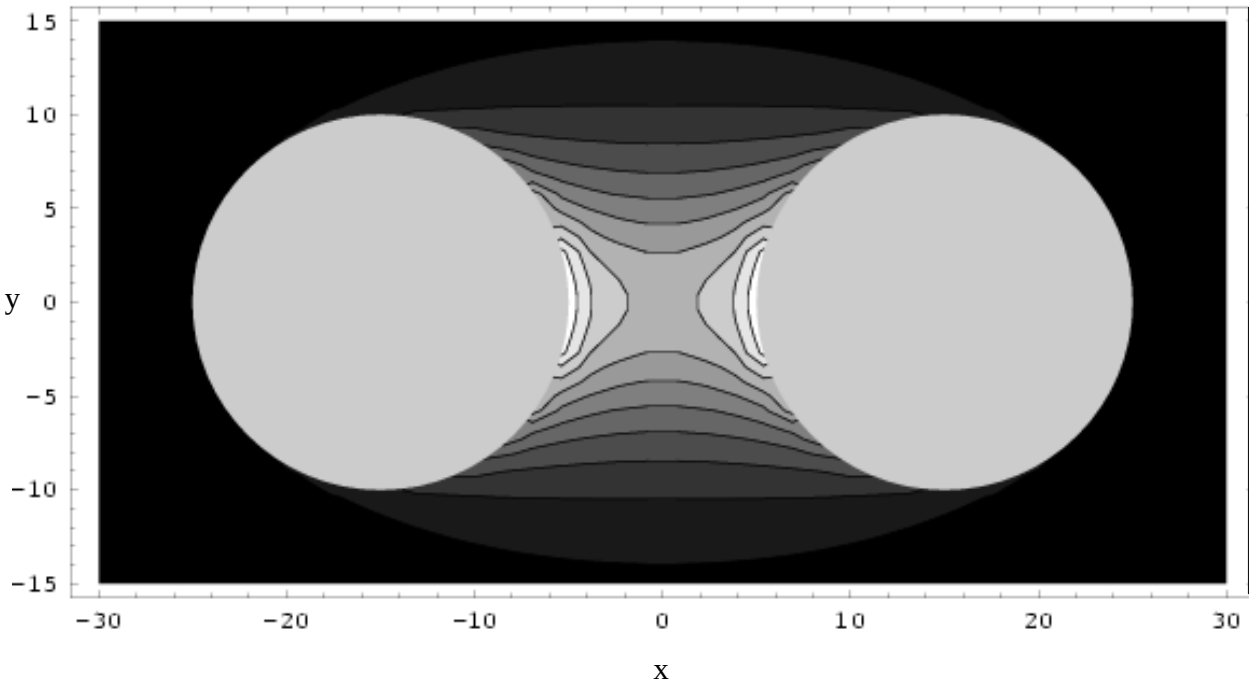

Fig. 2.— A contour plot of a slice through the stars of the angular dependence of the inter-star neutrino energy deposition density, Θ_{inter}, given by eqn. (9) with Eqns (11, 12), with stellar radii 10 km and separation 30 km. There are ten 1.1 increment contours starting from black, (0,1.1), and increasing to white. The neutron stars are represented by grey disks. This figure is meant to illustrate the function Θ_{inter} and thus does not include eclipsing of neutrino paths by the neutron stars which would attenuate this function around the far sides of the neutron stars. Since the effect is already small in these regions, this modification is negligible.

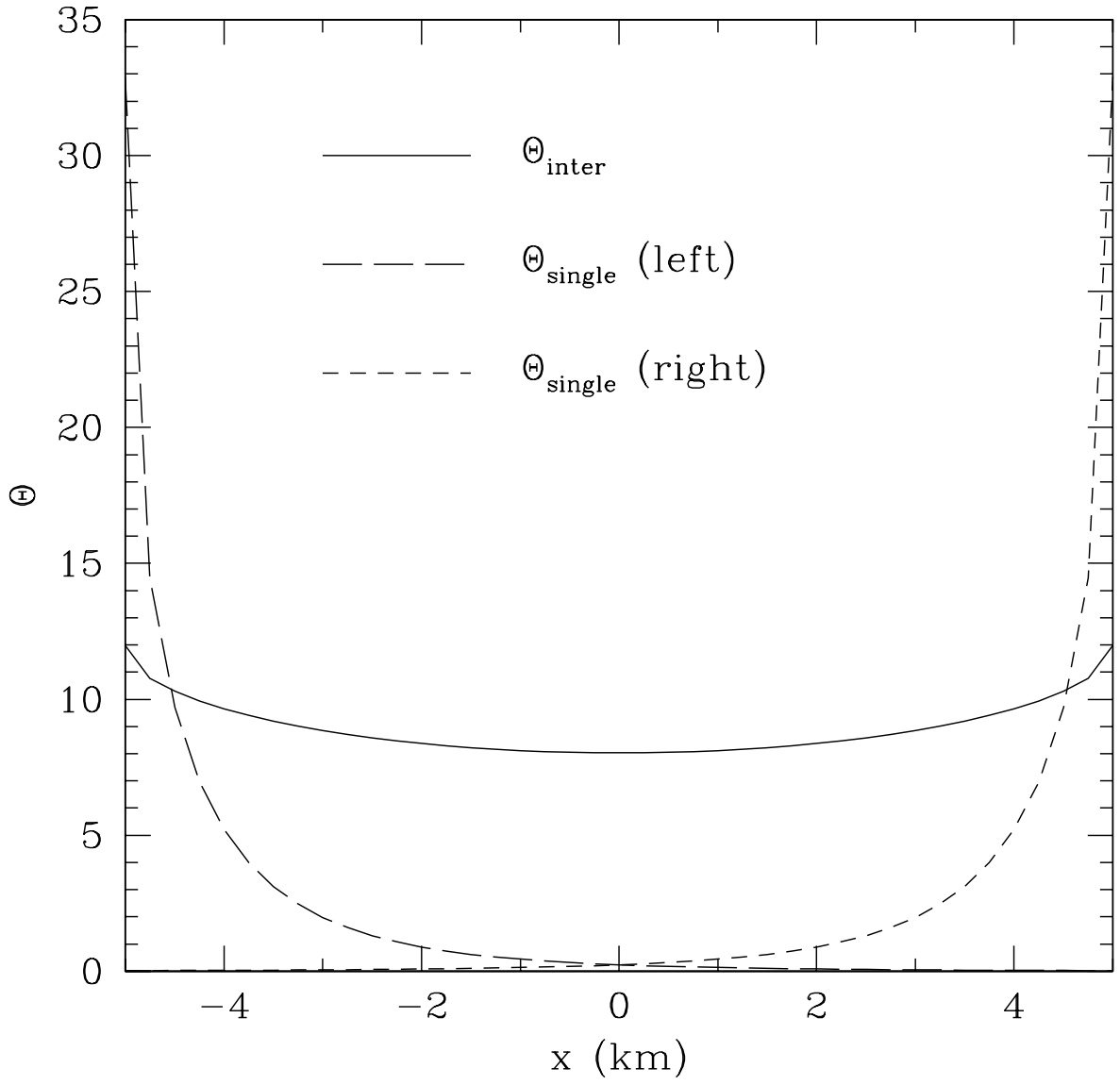

Fig. 3.— A plot of the region between the two neutron stars along the line connecting the two star centers. The left (right) edge of the plot is the surface of the left (right) star. The solid line is the inter-star deposition $\Theta_{\rm inter}$ given by Eqn (9, 11, 12) and shown also in Figure 2. The dashed lines are the single star angular deposition functions $\Theta_{\rm single}$ (Eqn. 13, 14, Newtonian; $M = 0$) for each star of radius 10 km and separation 30 km. Note that $\Theta_{\rm single}$ decays rapidly with distance from the surface of each neutron star while $\Theta_{\rm inter}$ is more gradually varying between the stars.

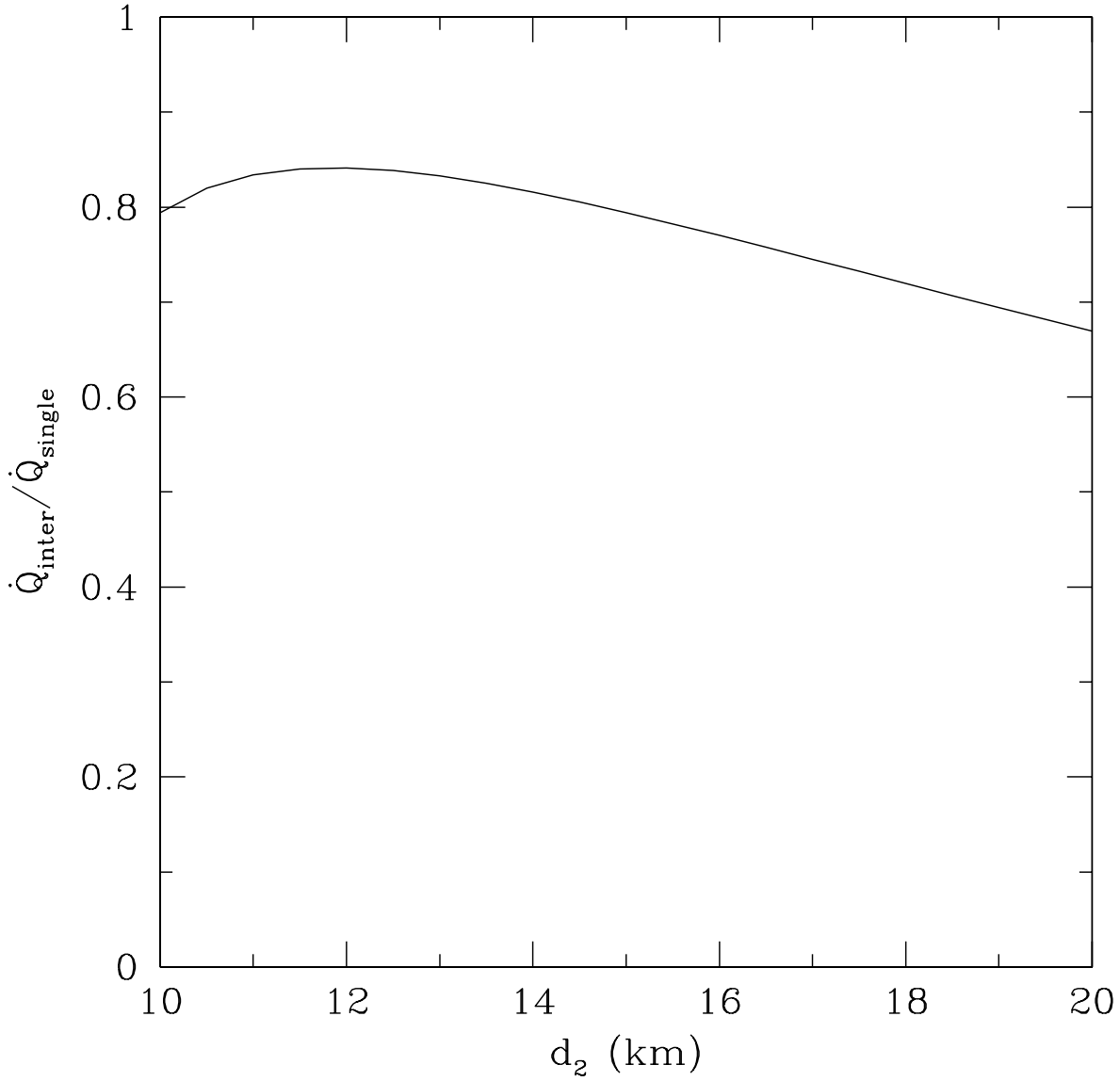

Fig. 4.— Ratio of integrals over space of inter-star energy angle factor (Eqns 9, 11, 12) to single star angle factor (Eqns 13, 14, Newtonian; $M = 0$). This is evaluated for star radii 10 km over a range of half-distances, d_2, between the star centers. The turn-down for small separations ($d_2 < 12$ km) is due to the paucity of volume between the stars.

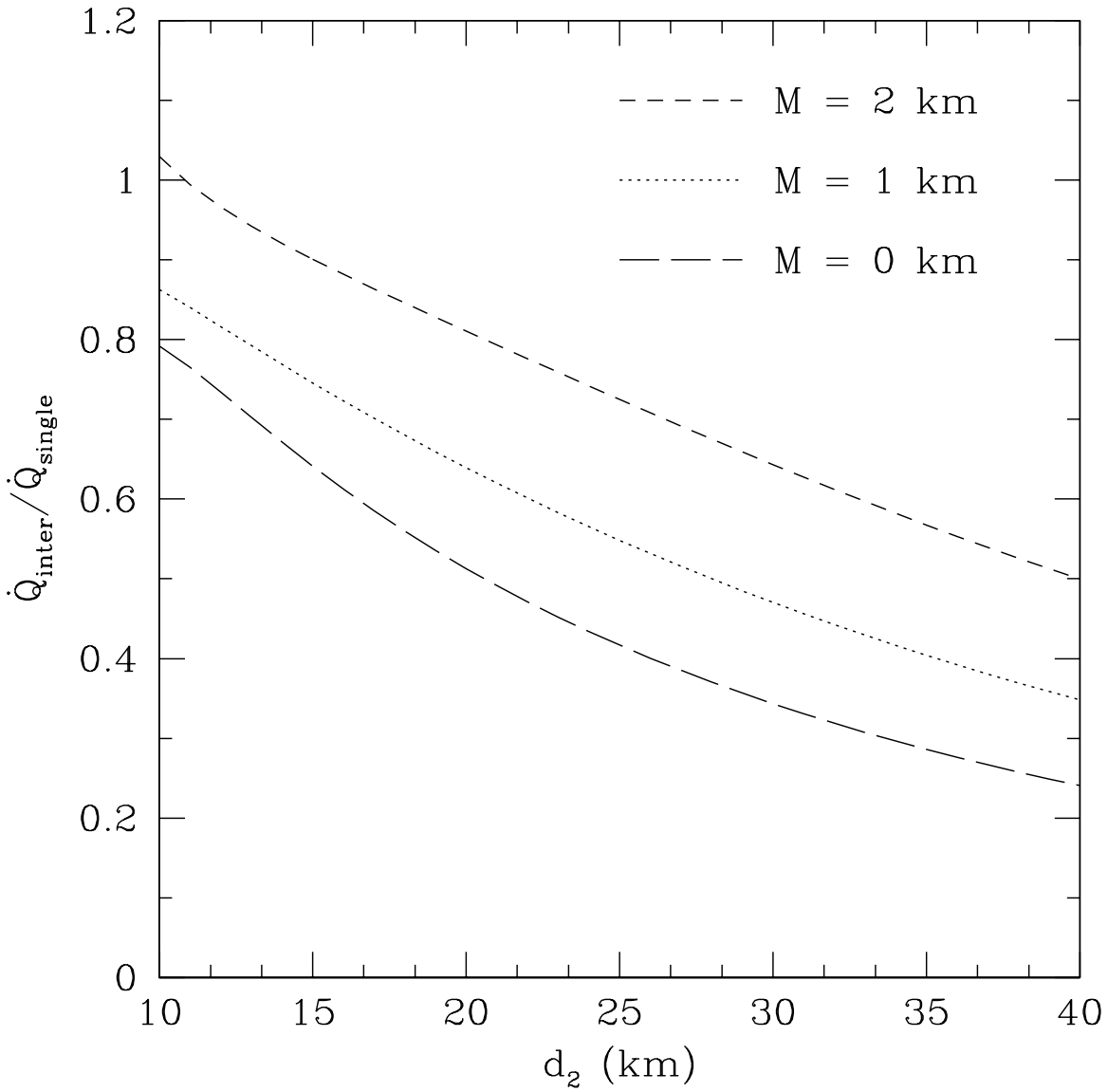

Fig. 5.— A ratio of the entire energy deposition due to inter-star neutrino annihilations, $\dot{Q}_{\rm inter}$, to that from single star annihilations, $\dot{Q}_{\rm single}$, is shown for isotropic stellar radii $\overline{R} = 7.5$ km for a range of stellar half-separations, d_2, and for several stellar masses M. $M = 0$ corresponds to the Newtonian, zero-gravity case. Note that for $M = 2$ km $\approx 1.4 M_\odot$ and $d_2 = 10$ km inter-star energy deposition, $\dot{Q}_{\rm inter}$, equals single star energy deposition $\dot{Q}_{\rm single}$.

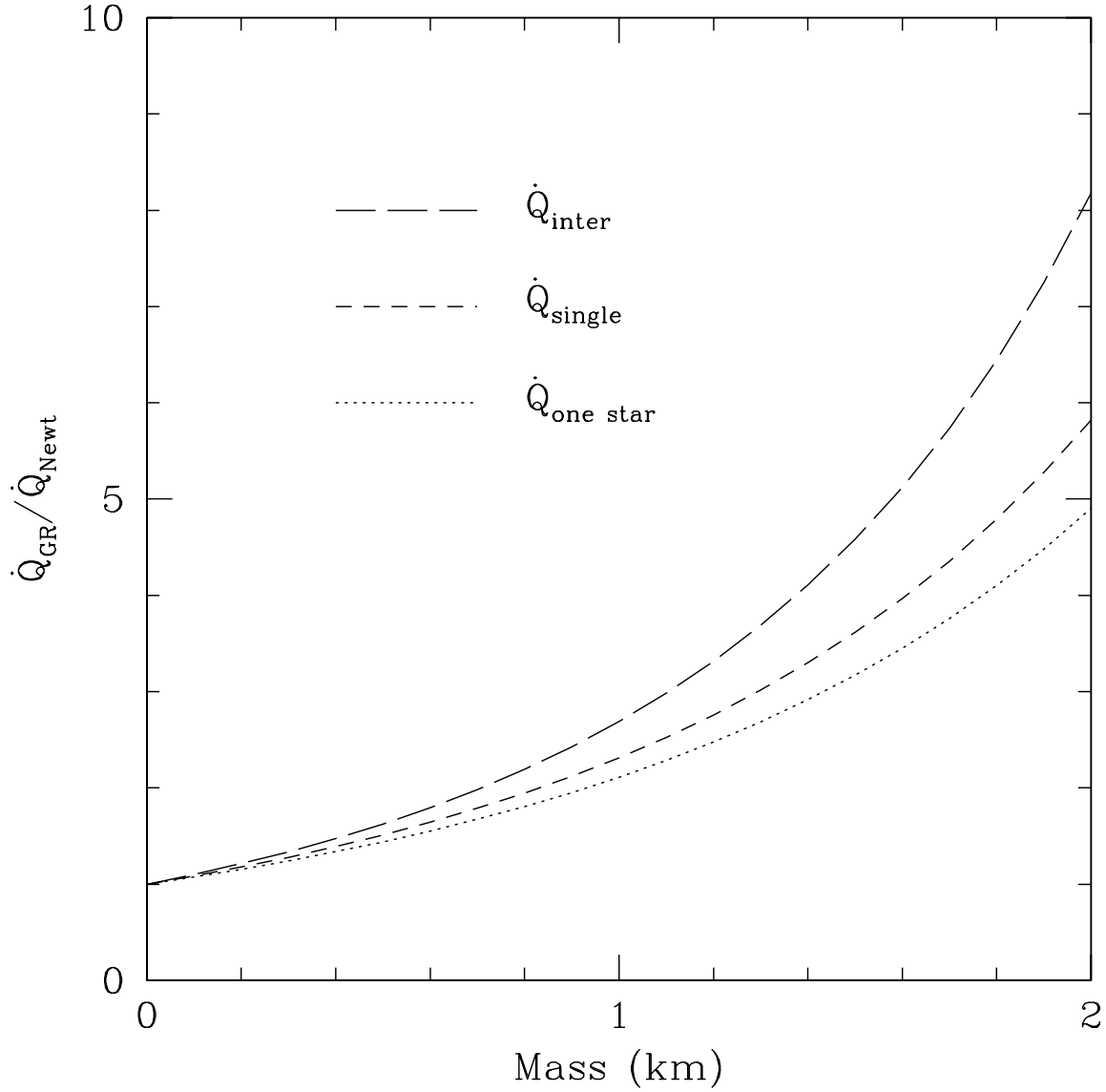

Fig. 6.— A comparison of the ratio $\dot{Q}_{\rm GR}/\dot{Q}_{\rm Newt}$ of general relativistic (eqn. 26) to Newtonian (eqn. 15) energy deposition. This ratio is shown for inter-star $\dot{Q}_{\rm inter}$ and single star $\dot{Q}_{\rm single}$ energy depostions for a range of stellar masses and with isotropic stellar radius $\overline{R} = 7.5$ km and half-separation $d_2 = 15$ km. As mass increases, both components are augmented by relativistic effects. For reference, the energy deposition is shown for an isolated neutron star, $\dot{Q}_{\rm one\ star}$, i.e. the same as $\dot{Q}_{\rm single}$, but with the companion star mass set to zero. The depositions in a binary system ($\dot{Q}_{\rm inter}$, $\dot{Q}_{\rm single}$) are augmented over $\dot{Q}_{\rm one\ star}$ because of the deeper, two-star potential well.